GEOS 38600/ GEOS 28600

Lecture 11

Wednesday 15 Feb 2017

The flow of ice

The flow of ice

ICE MOVEMENT – GLEN'S LAW

TEMPERATURE STRUCTURE WITHIN ICE SHEETS – ESKERS

EFFECT OF GLACIAL EROSION ON TOPOGRAPHY

Not covered today: water-ice moons (because the surface temps. are so low that the ice is brittle, away from rare cryovolcanoes)

Glaciers on Mars: debris covers protect 10^8-10^9 yr old ice

thickness of debris cover <10 m

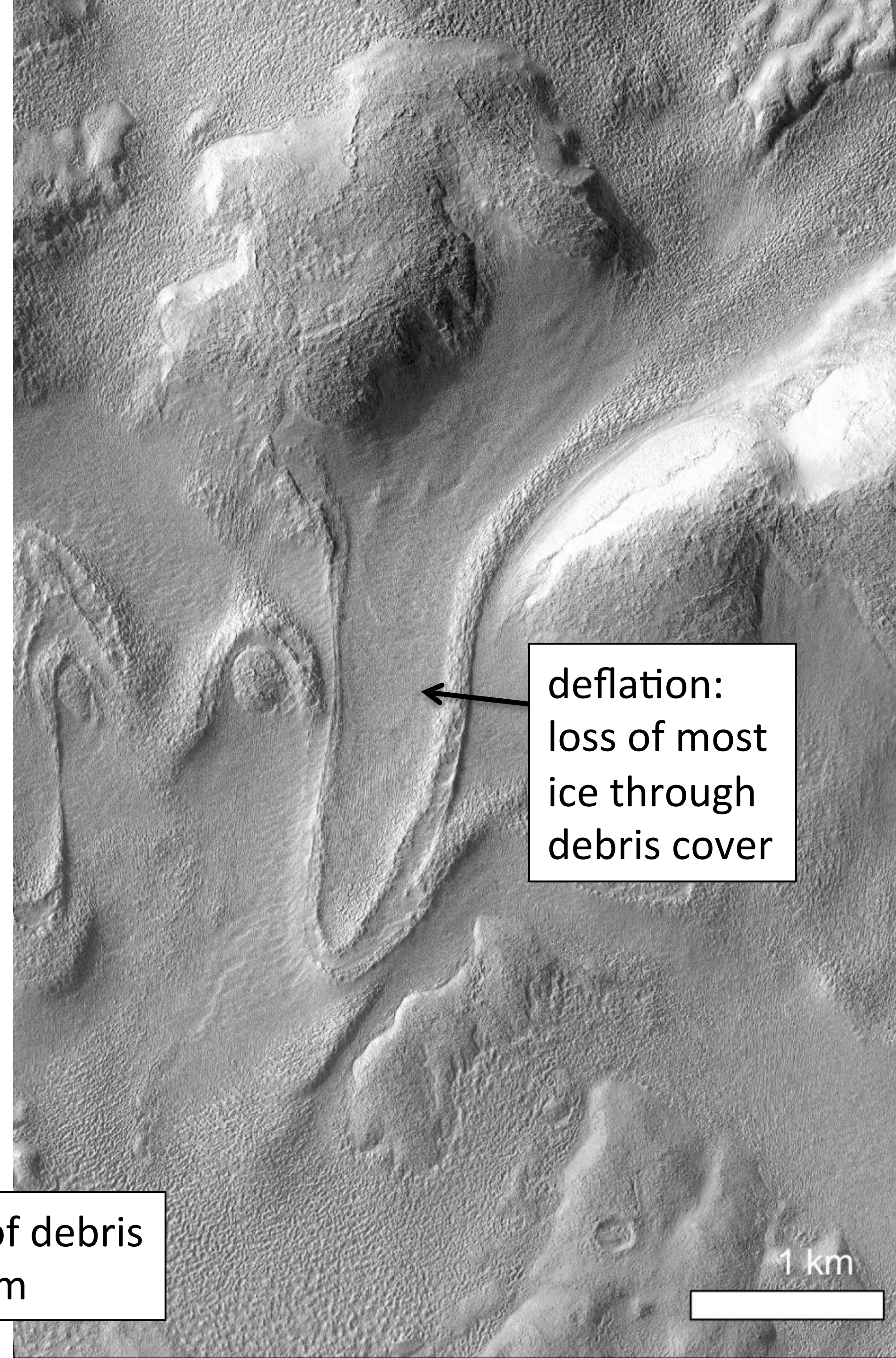

Nitrogen glaciers of Sputnik Planum (Pluto)

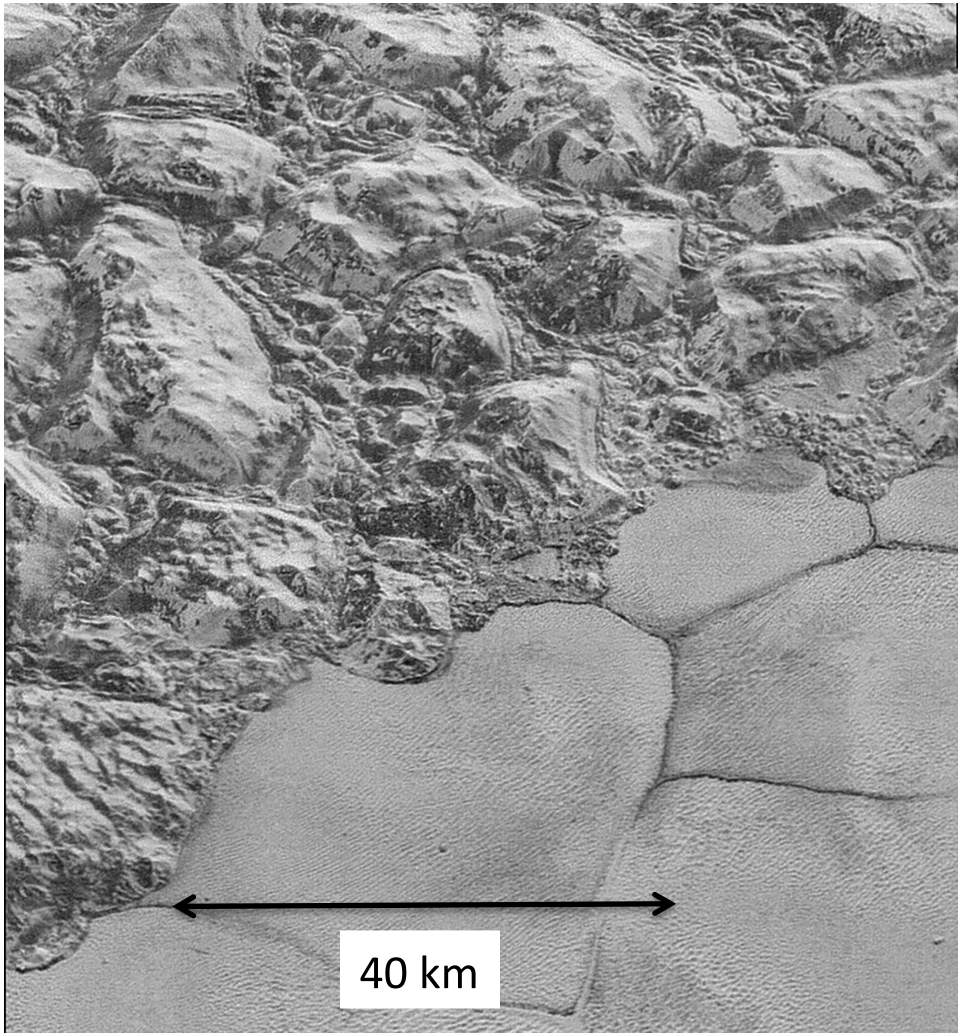

Water-ice mountains are 3 km high
Pluto surface temperature ~40 K

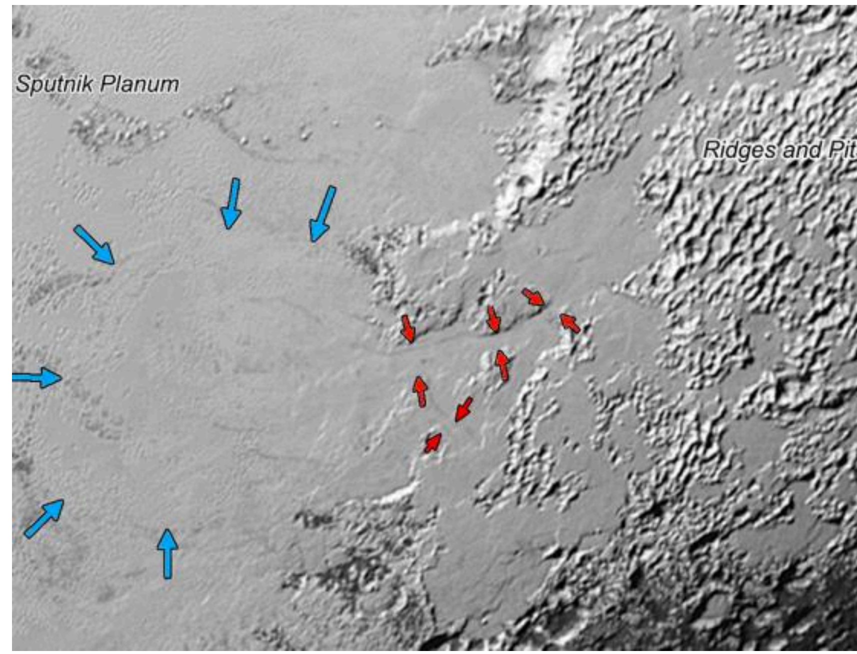

100km

e.g. see Umurhan et al. Icarus 2017 (suggested reading)

The topographic signature of glacial erosion of rock on Earth: "glacial buzzsaw"

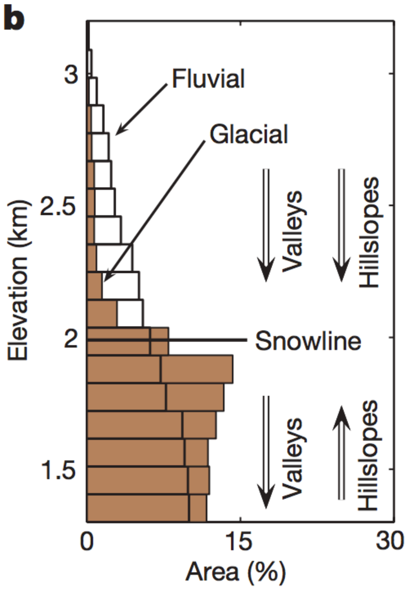

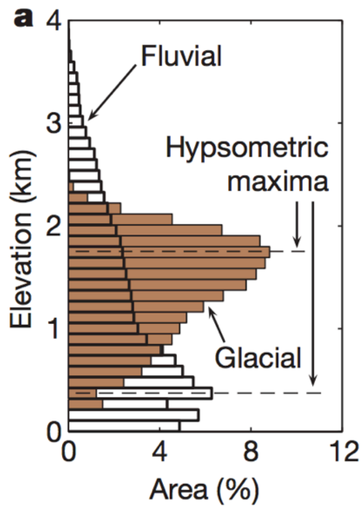

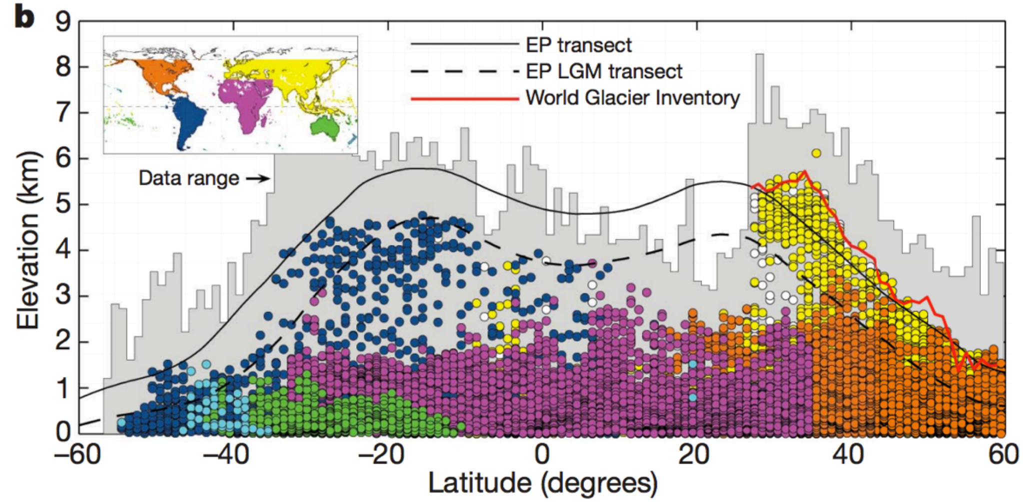

Hypsometric maxima for 60km x 60km areas

Egholm et al. Nature 2009

Gamburtsev mountains: today 3 km under Antarctic ice (nucleus for the Antarctic ice sheet, buried 33.7 Ma)

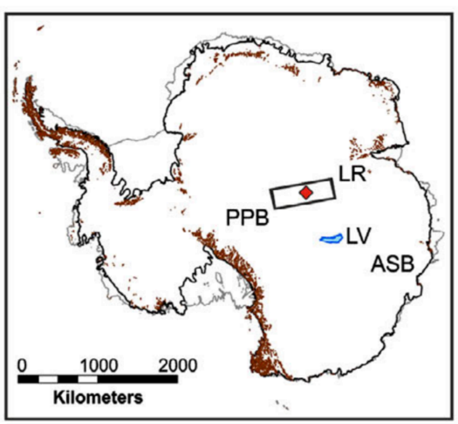

Radar mapping of buried paleo-topography

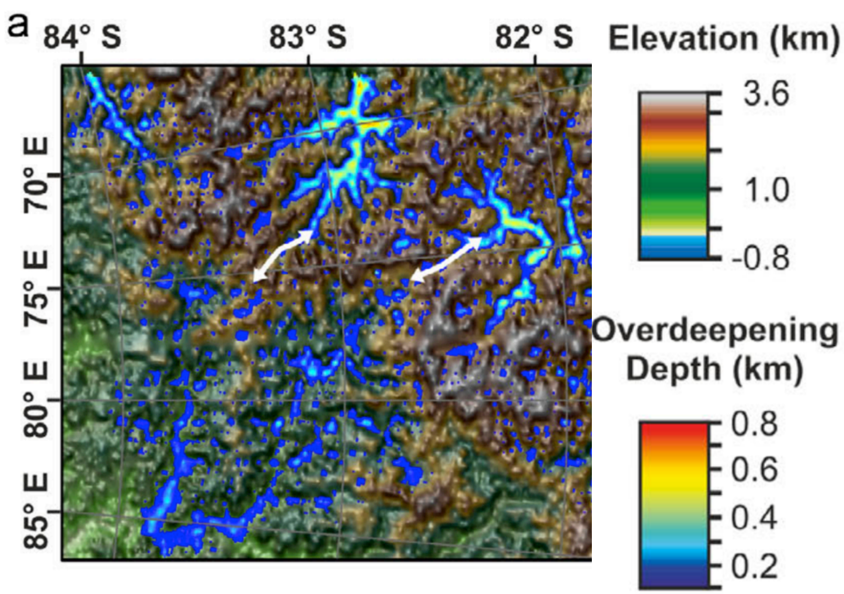

Positive feedbacks on ice sheet growth: albedo, elevation → adiabatic lapse rate

Ancient cirques preserved by <u>cold-based</u> ice

Rose et al. EPSL 2013

Ice flow physics will determine how fast Antarctica melts

Lifetime of anthropogenic CO2 in atmosphere: 10s of Kyr
Worst case for Antarctic melting (no geoengineering): centuries
Reasonable central guess: a few thousand years.

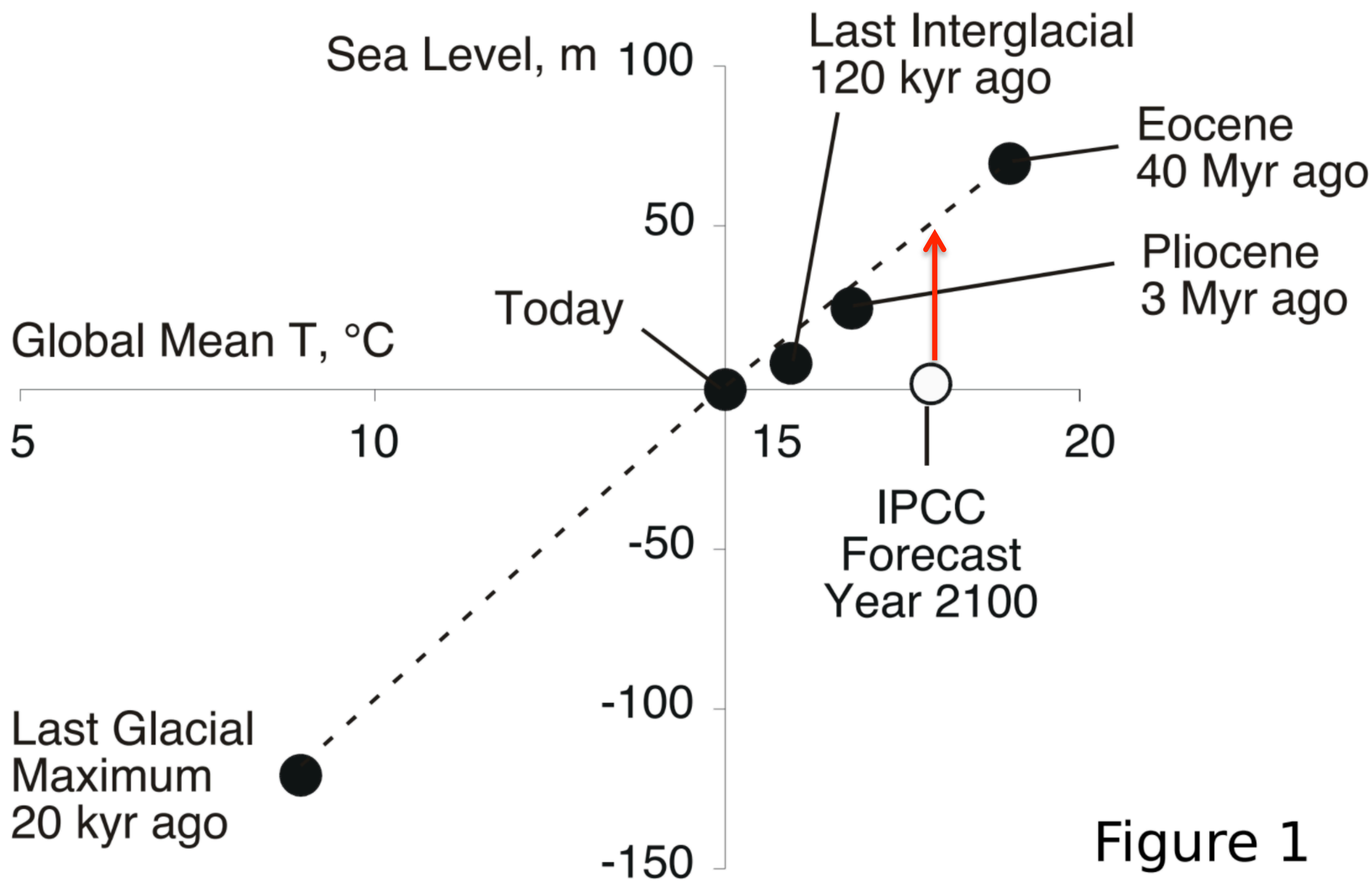

Figure 1

Archer & Kite, "The ultimate social cost of carbon", in prep.

Key points from today's lecture

- Glen's Law
- Approximations to the full Stokes equation: locations where they are and are not acceptable
- Nondimensional T-vs-depth as a function of accumulation rate for fixed basal heat flow
- Glacial erosion parameterization

The flow of ice

ICE MOVEMENT – GLEN'S LAW

TEMPERATURE STRUCTURE WITHIN ICE SHEETS – ESKERS (Mars examples)

EFFECT OF GLACIAL EROSION ON TOPOGRAPHY

(Earth examples)

Climate drives accumulation+ablation patterns, which drive glacial flow

Therefore**, changes in glacier length** (recorded by e.g. moraines, historical photographs) can be a proxy for **changes in climate.**

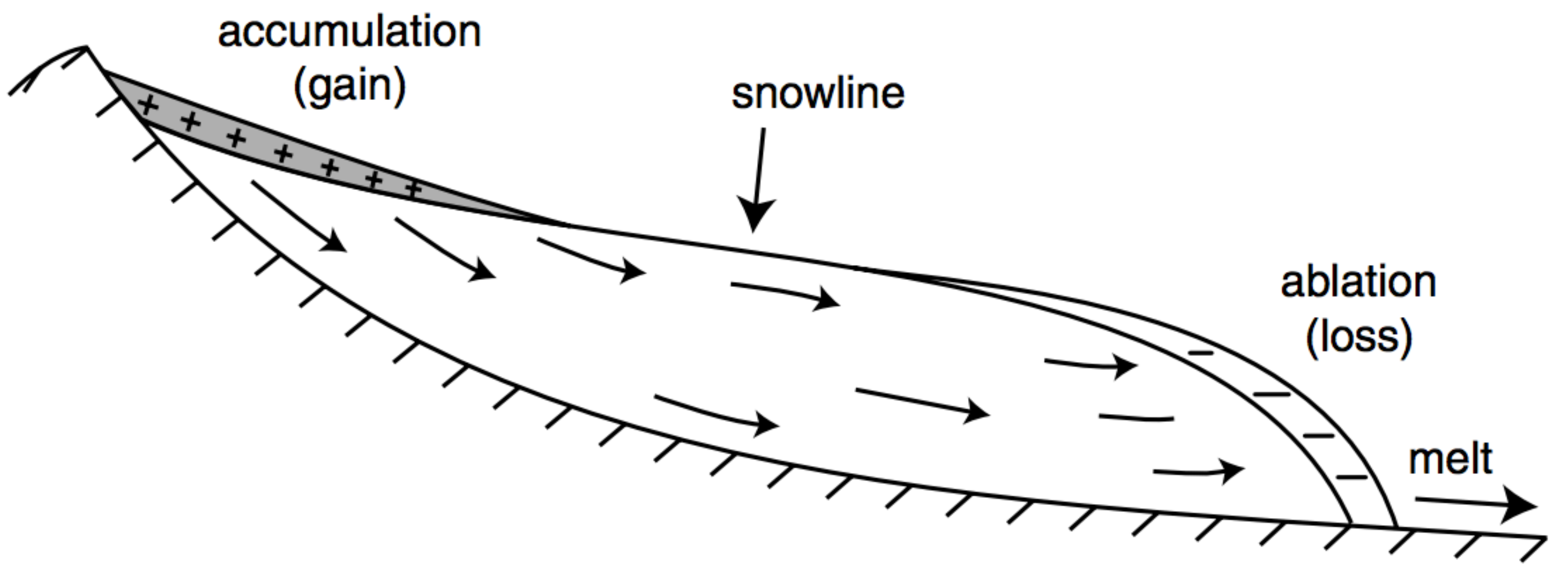

Mass balance on Earth favors ice accumulation at high elevations.

Orographic precipitation; low temperatures disfavor melting + sublimation

Mass balance on Mars *may* favor ice accumulation at low elevations.

Sublimation rate increases as pressure decreases

$$E_b = 0.17 D \rho_w (1 - r)\left(\frac{\Delta\rho}{\rho_a}\frac{g}{\nu^2}\right)^{\frac{1}{3}}$$

a)

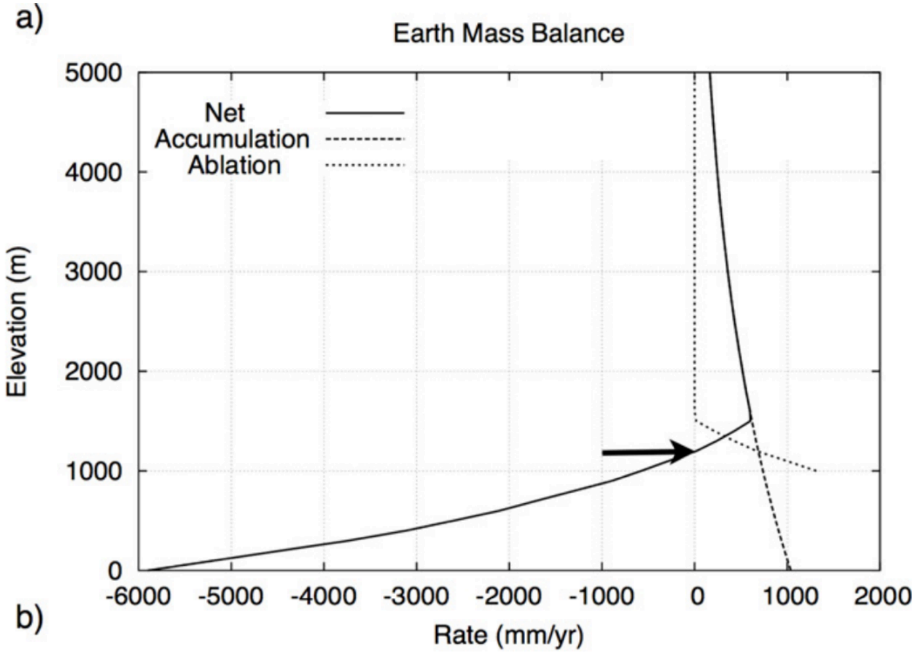

b)

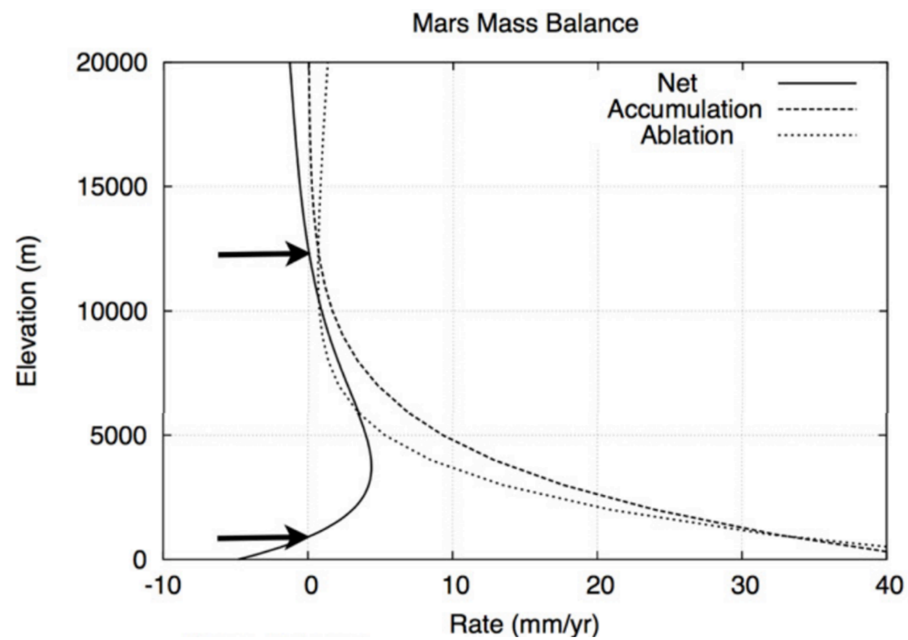

Fastook et al., Icarus 2008

Review of stress and strain

Definitions (2D – real case is 3D):

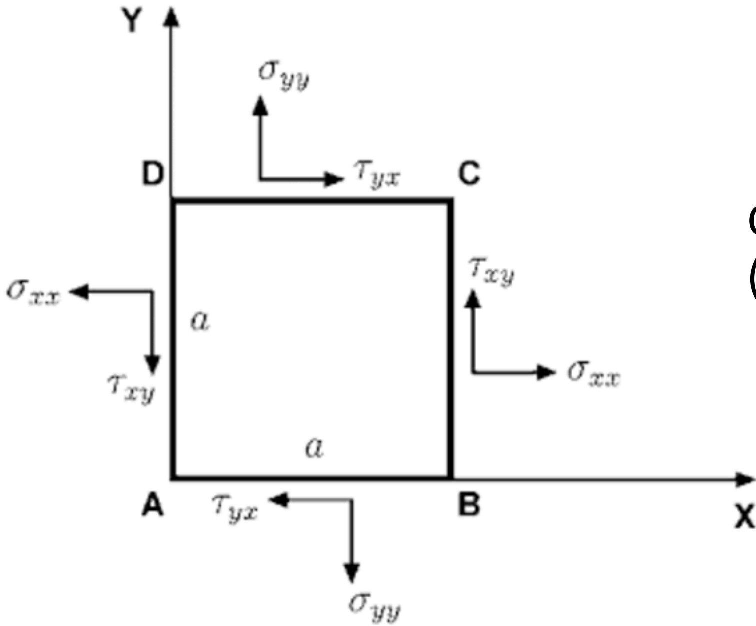

Assumption: Forces are balanced
(no rotational acceleration nor lateral acceleration)
<u>Infinitesimal</u> strain (invalid for complexly folded ice)

Convention: Extensional stresses defined as +ve
(note: in some engineering contexts, compression is +ve)

Rotate coordinate system to maximize normal stresses (these are then called the principal stresses)

Subtract off pressure:

$$\sigma_M = \frac{1}{3}[\sigma_1 + \sigma_2 + \sigma_3] = \frac{1}{3}[\sigma_{xx} + \sigma_{yy} + \sigma_{zz}]$$

$$\tau_{xx} = \sigma_{xx} - \sigma_M = \frac{1}{3}[2\sigma_{xx} - \sigma_{yy} - \sigma_{zz}]$$

$$\left[\frac{\partial \sigma_{xx}}{\partial x}\delta x\right]\delta y + \left[\frac{\partial \tau_{xy}}{\partial y}\delta y\right]\delta x.$$

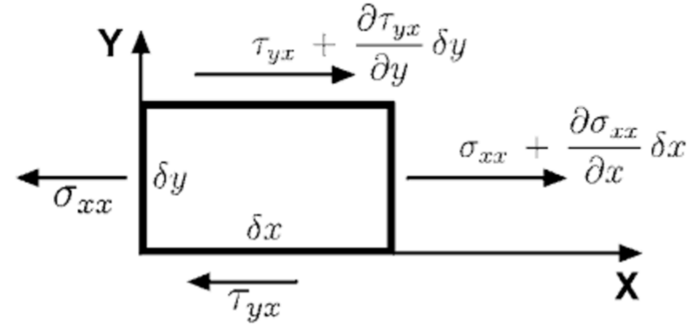

Ice is incompressible, so only deviatoric stresses matter for flow

0 - Pressure:

Ice flow is pressure-independent for pressure within glaciers

$$\sigma_{\mathrm{M}} = \frac{1}{3}\left[\sigma_{xx} + \sigma_{yy} + \sigma_{zz}\right].$$

$$\begin{pmatrix} \tau_{xx} & \tau_{xy} & \tau_{xz} \\ \tau_{xy} & \tau_{yy} & \tau_{yz} \\ \tau_{xz} & \tau_{yz} & \tau_{zz} \end{pmatrix} = \begin{pmatrix} \sigma_{xx} - \sigma_{\mathrm{M}} & \sigma_{xy} & \sigma_{xz} \\ \sigma_{xy} & \sigma_{yy} - \sigma_{\mathrm{M}} & \sigma_{yz} \\ \sigma_{xz} & \sigma_{yz} & \sigma_{zz} - \sigma_{\mathrm{M}} \end{pmatrix}$$

Effective stress:

$$\tau_{\mathrm{E}}^2 \equiv \frac{1}{2}\left[\tau_{xx}^2 + \tau_{yy}^2 + \tau_{zz}^2\right] + \tau_{xz}^2 + \tau_{xy}^2 + \tau_{yz}^2.$$

Pure shear vs. simple shear

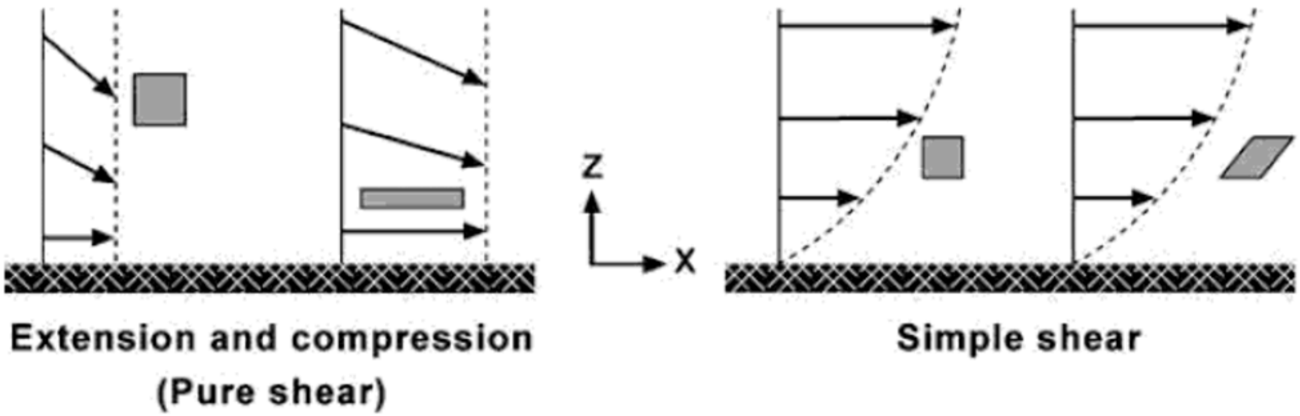

$$\dot{\epsilon}_{xx} = -\dot{\epsilon}_{zz}$$

$$\dot{\epsilon}_{xz} = \dot{\epsilon}_{zx} = 0.$$

$$\dot{\epsilon}_{xz} = \dot{\epsilon}_{zx} \neq 0$$

$$\dot{\epsilon}_{xx} = \dot{\epsilon}_{zz} = 0$$

Stress → strain: rheology of water ice near 273K

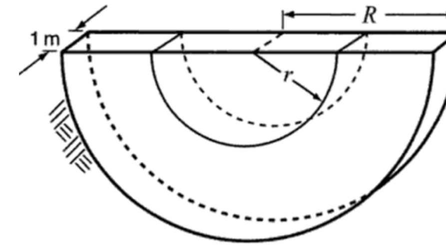

Dislocation creep:

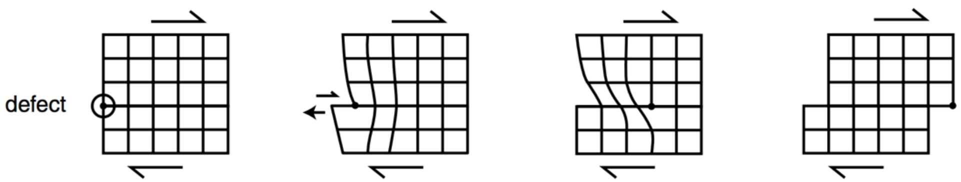

in practice "regularized"

Glen's Flow Law

$$\dot{\epsilon}_{xy} = A\tau_{xy}^{n}$$

n = approximately 3

$$A = A_0 \exp(-Q/RT)$$

Q ~ 60 kJ/mol

$$\dot{\epsilon}_{jk} = A\,\tau_{\mathrm{E}}^{n-1}\,\tau_{jk}$$

Nye-Glen law for incompressible, isotropic ice

"toothpaste tube" limit

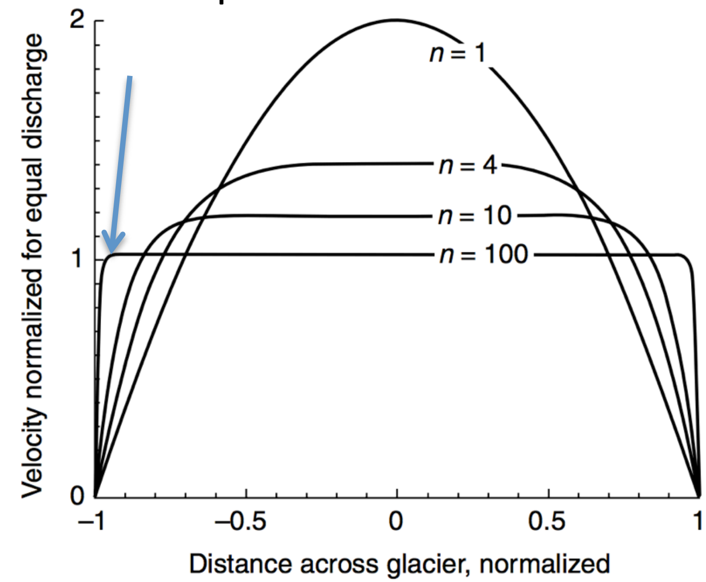

$$u_z(r) = \frac{2A}{n+1}(\rho g \sin\alpha)^n \left[\left(\frac{R}{2}\right)^{n+1} - \left(\frac{r}{2}\right)^{n+1}\right].$$

Semicircular channel, radius R

Effects of grain orientation and grain size can be important (but less so than the stress and temperature effects)

Strong temperature dependence and strong shear-stress dependence

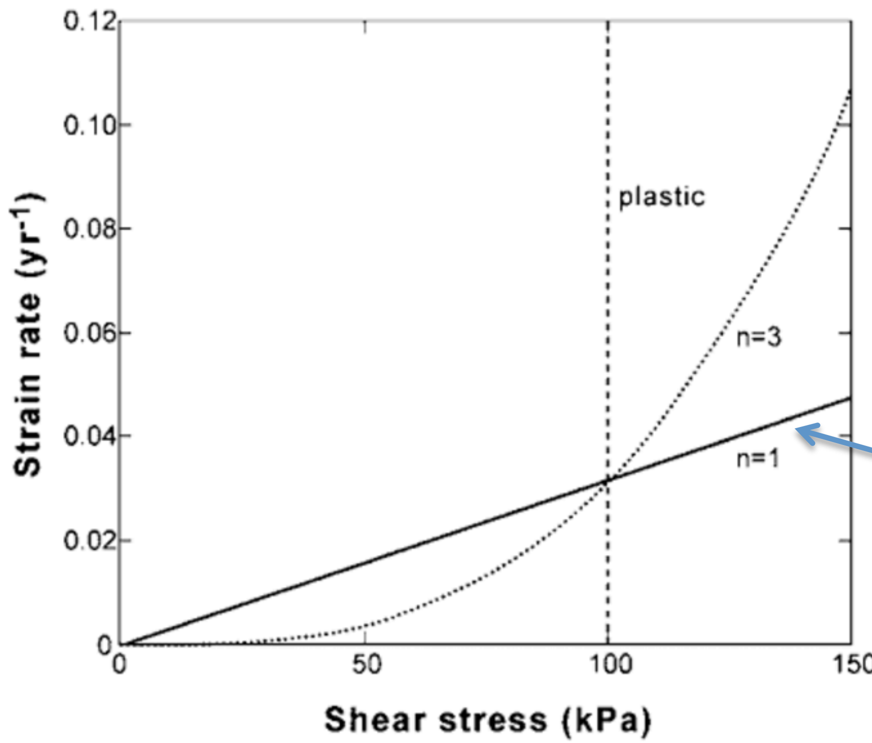

10^{14} Pa s

Effective viscosity decreases as shear stress increases

$$\eta = \frac{1}{2}\left[A\,\tau_{\mathrm{E}}^{n-1}\right]^{-1}$$

Stress: which components of stress to consider?

neglects longitudinal and transverse stresses

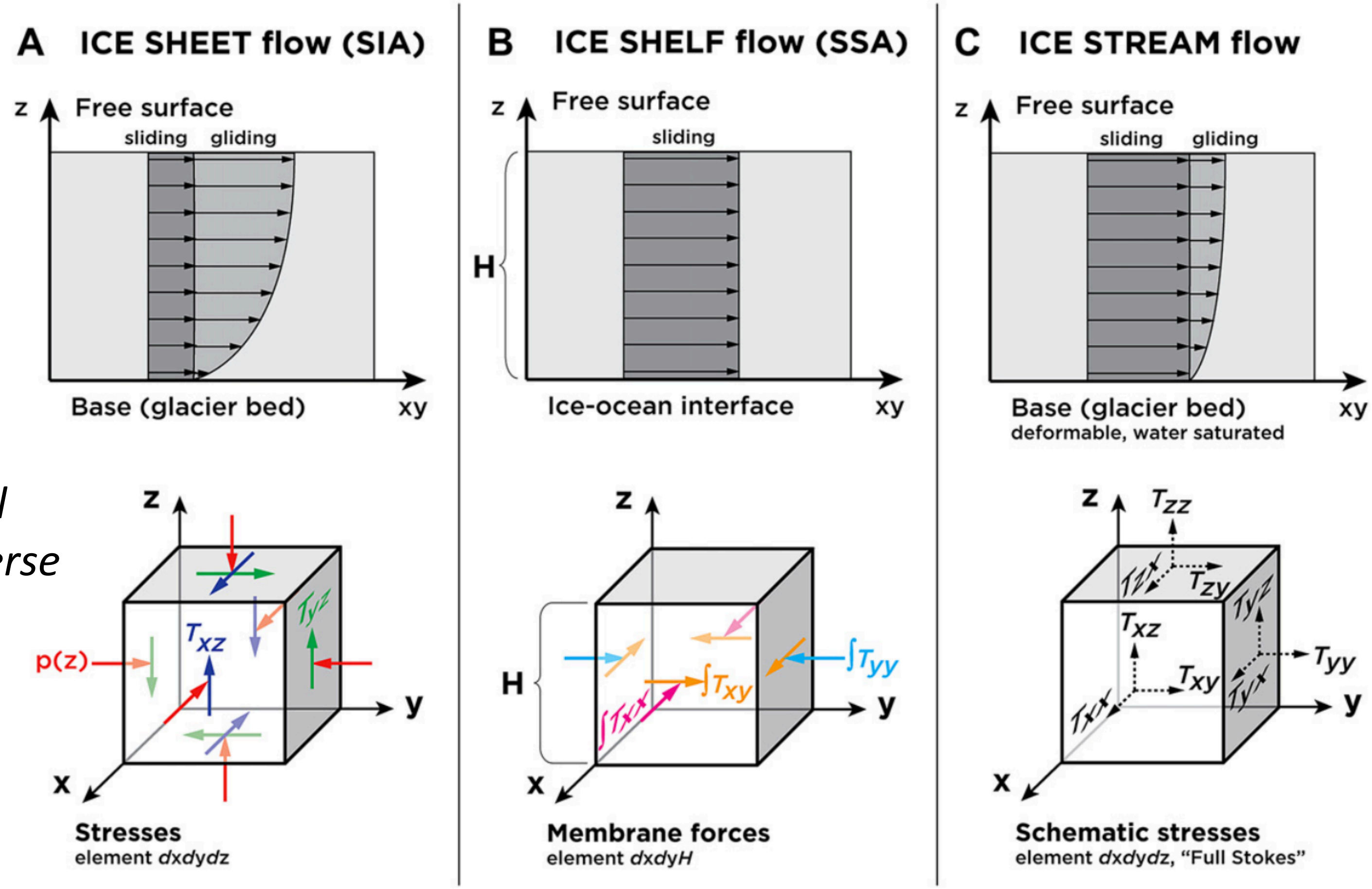

Fig. 4. Velocity profiles and stress states. Schematic visualization of characteristic velocity profiles (top row) and stress components (bottom row) arising in ice sheet (A), ice shelf (B) and ice stream (C) flow, cf. cubes A, B and C in Fig. 2. A) Velocity profile in the SIA (ice sheet flow), resulting from sliding at the base and gliding due to internal deformation. Flow is dominated by (xy) -parallel shearing stresses T_{xz} and T_{yz}. The element $dxdydz$ has z -dependent cryostatic pressure $p(\cdot,z)$ and shear stress distributions $T_{xz}(\cdot,z), T_{yz}(\cdot,z)$. The indicated stress components are the only ones retained in a zero order model. B) Vertically uniform horizontal velocity field in the SSA (ice shelf flow). This velocity field is induced by the depth-integrated (xy) -parallel normal and shear stresses $T^E_{xx}, T^E_{yy}, T^E_{xy}$. The integrated stress components are often referred to as membrane forces as illustrated for an element $dxdyH$ ($H =$ ice shelf thickness, as in Fig. 1). C) Velocity profile (ice stream flow) with pronounced contributions from sliding, resembling a combined sheet- and shelf-flow profile. Employing all six stress components of the Cauchy stress tensor corresponds to a full Stokes approach. A proper scaling analysis for ice streams would reveal the relative importance of normal stresses T_{xx}, T_{yy}, T_{zz} and shear stresses T_{xy}, T_{xz}, T_{yz} ; i.e. which ones could be assigned weights ε^n, $n \geq 1$ without losing characteristic ice stream features.

SIA: Shallow Ice Approximation
SSA: Shallow Shelf Approximation

Kirchner et al.,
Quaternary Science Reviews 2011

Stress: which components of stress to consider?

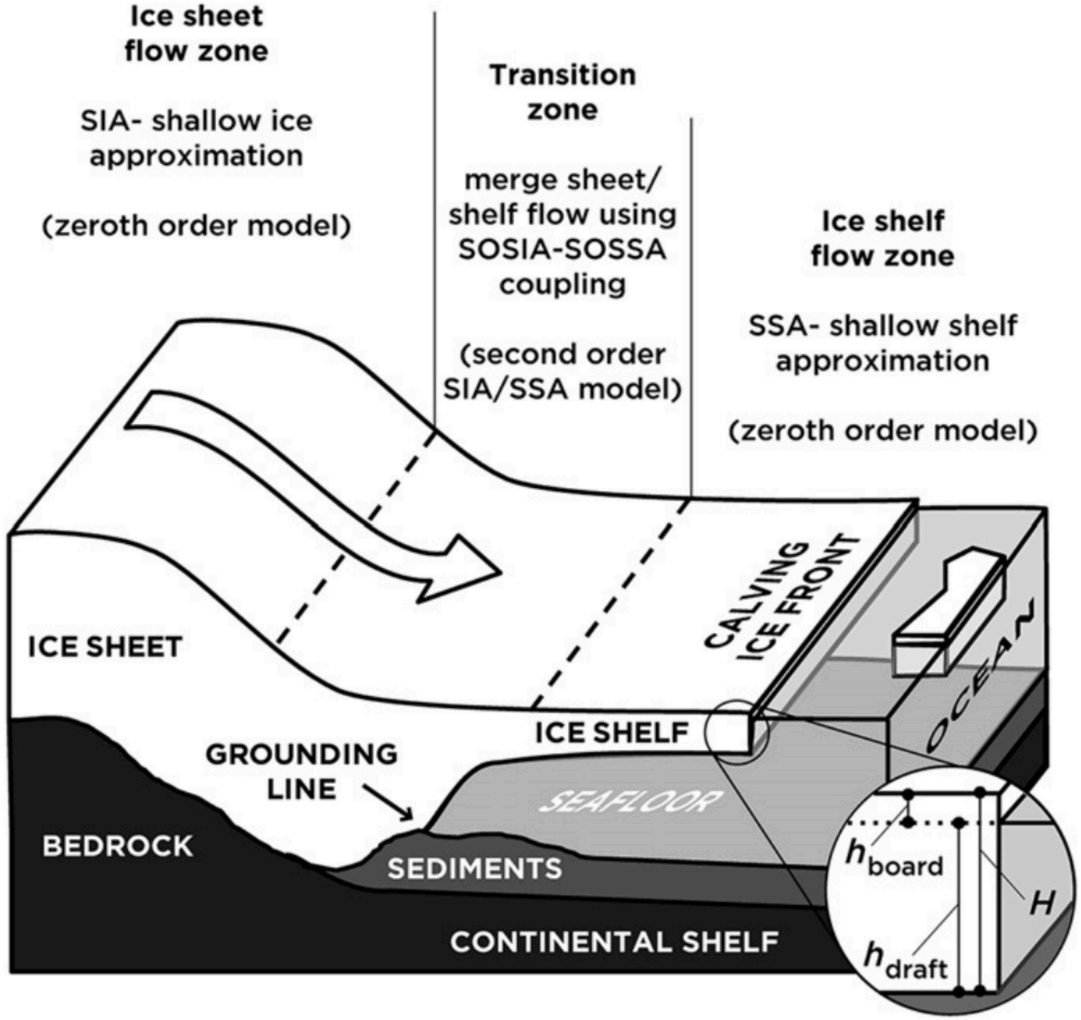

Fig. 1. Sketch of a coupled ice sheet-ice shelf system. In sufficient upstream (downstream) distance from the grounding line, pure ice sheet flow (ice shelf flow) is described by the zero order Shallow Ice Approximation SIA (zero order Shallow Shelf Approximation SSA). In a transition region across the grounding line, both sheet flow and shelf flow features prevail. There, SIA and SSA have to be extended before they can be coupled using the second order SO-SIA and SO-SSA modeling approaches.

Kirchner et al. 2011
Quaternary Science
Reviews

Stress: which components of stress to consider?

non-dimensionalized

SHALLOW ICE APPROXIMATION

$$
\text{(SIA)}\quad
\begin{aligned}
0 &= -\frac{\partial p_{(0)}}{\partial x} + \frac{\partial T^E_{xz(0)}}{\partial z} \\
0 &= -\frac{\partial p_{(0)}}{\partial y} + \frac{\partial T^E_{yz(0)}}{\partial z} \\
1 &= -\frac{\partial p_{(0)}}{\partial z}.
\end{aligned}
$$

SHALLOW ICE APPROXIMATION

$$
\text{(SSA)}\quad
\begin{aligned}
0 &= -\frac{\partial p_{(0)}}{\partial x} + \frac{\partial T^E_{xx(0)}}{\partial x} + \frac{\partial T^E_{xy(0)}}{\partial y} + \frac{\partial T^E_{xz(0)}}{\partial z} \\
0 &= -\frac{\partial p_{(0)}}{\partial y} + \frac{\partial T^E_{xy(0)}}{\partial x} + \frac{\partial T^E_{yy(0)}}{\partial y} + \frac{\partial T^E_{yz(0)}}{\partial z} \\
\frac{\rho_{sw}}{\rho_{sw} - \rho} &= -\frac{\partial p_{(0)}}{\partial z} + \frac{\partial T^E_{zz(0)}}{\partial z}
\end{aligned}
$$

floating

Vertically integrated force balance (map-plane models)

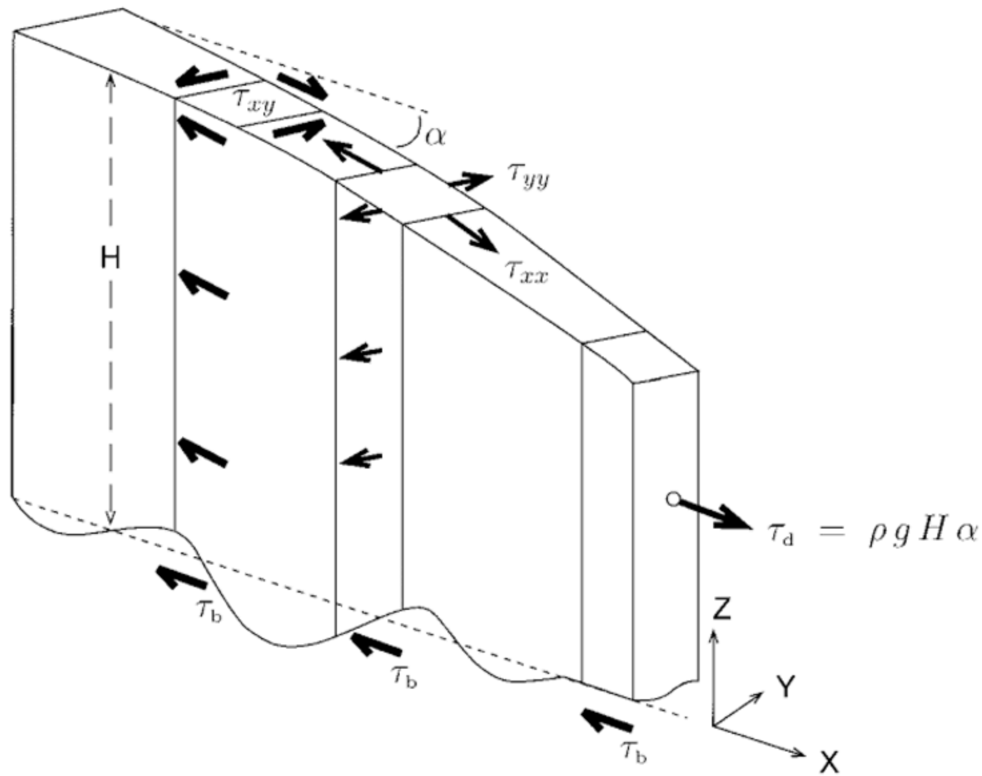

Cuffey & Patterson 2010
e.g. Fastook & Chapman, J. Glaciol., 1989

Plastic-flow approximation to ice sheet profiles (steady state)

Assume Y = 10^5 Pa (larger for cold ice)

$$H = \sqrt{\frac{2YL}{\rho g}}$$

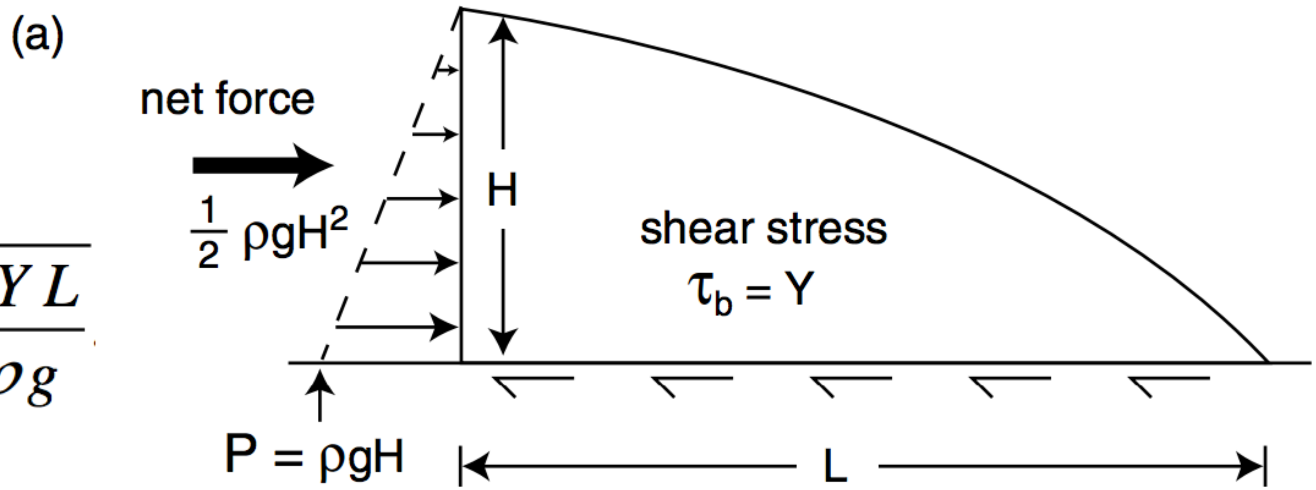

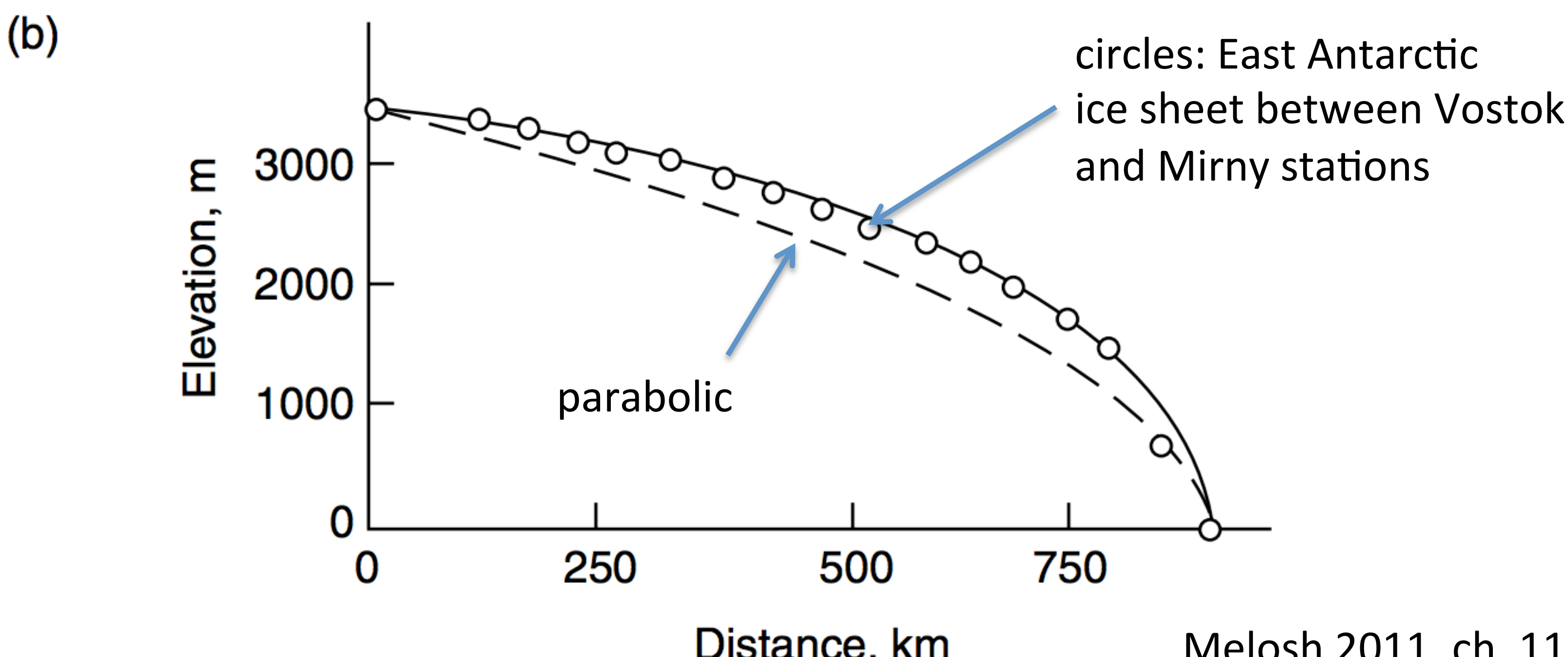

Melosh 2011, ch. 11

Example: how long to seal a system of crevasses?

Assume Glen's law

$$\sigma_{xx} = \sigma_o; \quad \sigma_{zz} = \sigma_o + \hat{\sigma}_z; \quad \dot{\epsilon}_{yy} = 0$$

$$\dot{\epsilon}_{xx} = -\dot{\epsilon}_{zz}; \quad \sigma_{yy} = \sigma_o + \frac{1}{2}\hat{\sigma}_z$$

$$\tau_{zz} = -\tau_{xx} = \frac{1}{2}\hat{\sigma}_z$$

$$\dot{\epsilon}_{zz} = \frac{1}{8} A\, \hat{\sigma}_z^3$$

Table 3.4: Recommended base values of creep parameter A at different temperatures and $n = 3$.

Error relative to ice-sheet data: factor of 3

T (°C)	A ($s^{-1}Pa^{-3}$)
0	2.4×10^{-24}
−2	1.7×10^{-24}
−5	9.3×10^{-25}
−10	3.5
−15	2.1
−20	1.2×10^{-25}
−25	6.8×10^{-26}
−30	3.7
−35	2.0
−40	1.0×10^{-26}
−45	5.2×10^{-27}
−50	2.6

Cuffey & Patterson 2010

An σ_{yy} value intermediate between σ_{xx} and σ_{zz} must exist to prevent extension in the y-direction. This stress system applies in an ice shelf occupying a bay; an ice stream with a weak bed; the upper layers of valley glaciers; and the upper layers in flank regions of ice sheets shaped like ridges.

The flow of ice

ICE MOVEMENT – GLEN'S LAW

TEMPERATURE STRUCTURE WITHIN ICE SHEETS + ESKERS (Mars examples)

EFFECT OF GLACIAL EROSION ON TOPOGRAPHY (Earth examples)

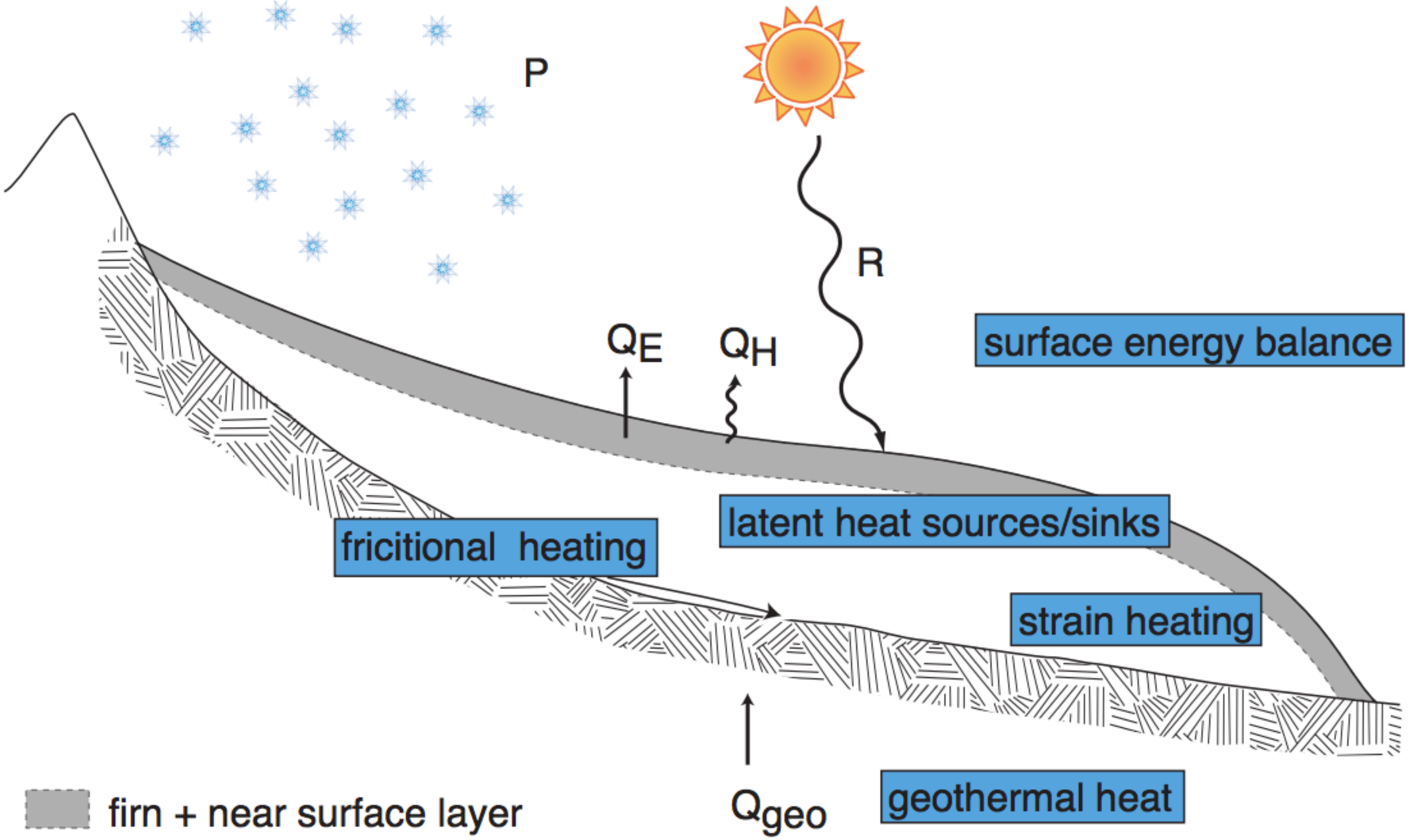

Andy Anschwanden, Glaciology Summer School

Decay of T signal of climate forcing with depth

$$T(z,t) = A_{\mathrm{T}} \exp\left(-z\sqrt{\pi\omega/\alpha_{\mathrm{T}}}\right) \sin\left(2\pi\omega t - z\sqrt{\pi\omega/\alpha_{\mathrm{T}}}\right).$$

a way to quantify exceptional late-20th warmth relative to earlier centuries

Table 9.1: Values for thermal parameters of pure ice.

		Temperature	
		0 °C	**−50 °C**
Specific heat capacity	$\mathrm{J\,kg^{-1}K^{-1}}$	2097	1741
Latent heat of fusion	$\mathrm{kJ\,kg^{-1}}$	333.5	
Thermal conductivity	$\mathrm{W\,m^{-1}K^{-1}}$	2.10	2.76
Thermal diffusivity	$10^{-6}\mathrm{m^2s^{-1}}$	1.09	1.73

Cuffey & Patterson, ch. 9 (supplementary reading)

Thermal structure of an ice sheet: neglecting horizontal advection

For slow-flowing ice sheets (e.g., Mars)
→ shear heating unimportant, temperature set by geothermal heat flow modified by advection of cold ice from above

surface mass balance: thickness/time

$$\gamma = \frac{\dot{b}_i H}{\alpha_\mathrm{T}}$$

signed Peclet number

$$\alpha_\mathrm{T} \frac{d^2 T}{dz^2} - w \frac{dT}{dz} = 0.$$

Constant heat flow at $z = 0$
(Geothermal + shear heating)
Mass removed at bed
(e.g., rapid lateral flow)
(Ice divide)

$$\xi = \frac{z}{H}$$

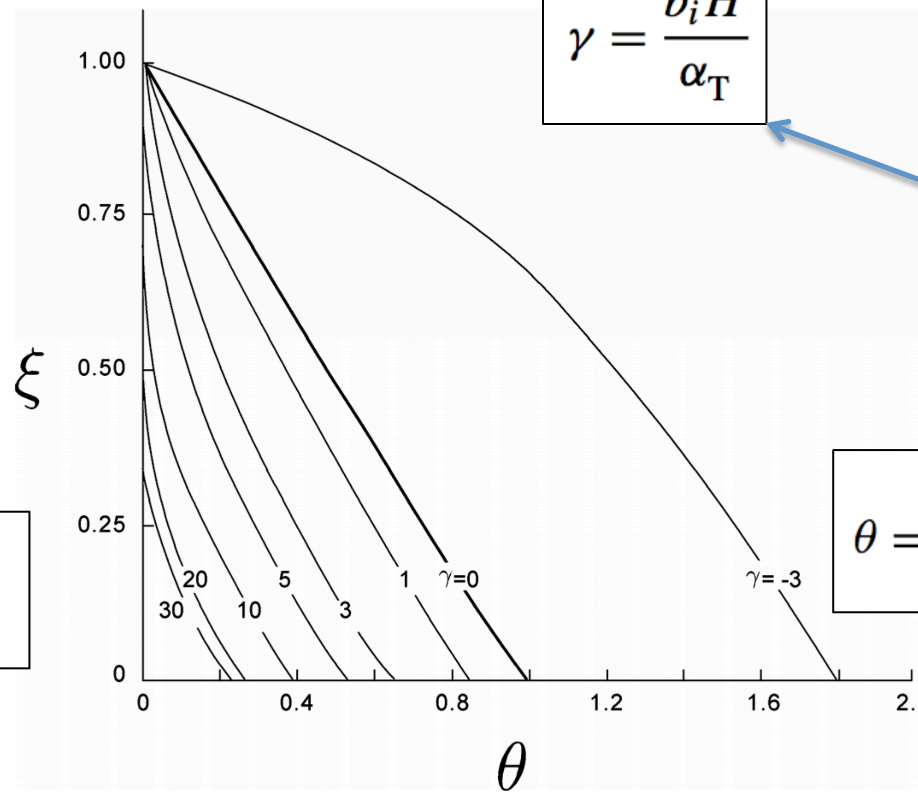

$$\theta = \frac{k_\mathrm{T}\,[T - T_s]}{GH}$$

Figure 9.5: Dimensionless steady temperature profiles for various values of the advection parameter (γ). Negative value for γ indicates upward velocity; positive values indicate downward velocity. Equations 9.19–9.21 define the variables; θ refers to scaled temperature and ξ to scaled height above the bed. Adapted from Clarke et al. (1977) and used with permission of the American Geophysical Union, *Reviews of Geophysics and Space Physics*.

Cuffey & Patterson, ch. 9 (supplementary reading)

Linking thermal structure and ice flow: crevasse-closure regulation of the rate of volcanism on Enceladus?

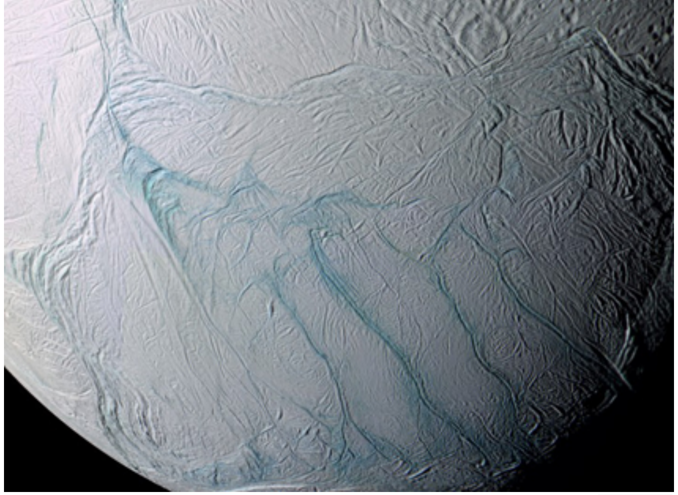

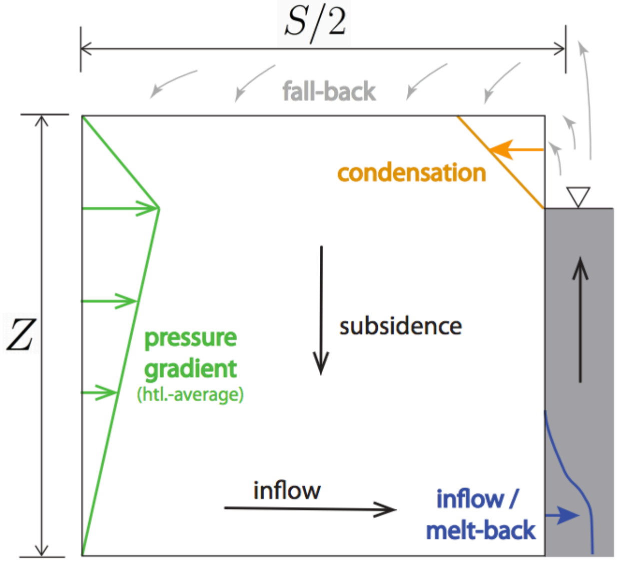

Figure S6. Long-lived liquid-water slots (that are in isostatic balance with adjacent ice) set up differential stresses (green arrows show vertical gradient in horizontally-averaged differential stress) that drive flow in the adjacent ice shell. Removal of ice by inflow and slot melt-back is compensated by subsidence. Subsidence provides accommodation space for condensation of vapor and for ballistic fall-back of erupted ice particles (materials that would otherwise seal the slot, powering down the eruptions).

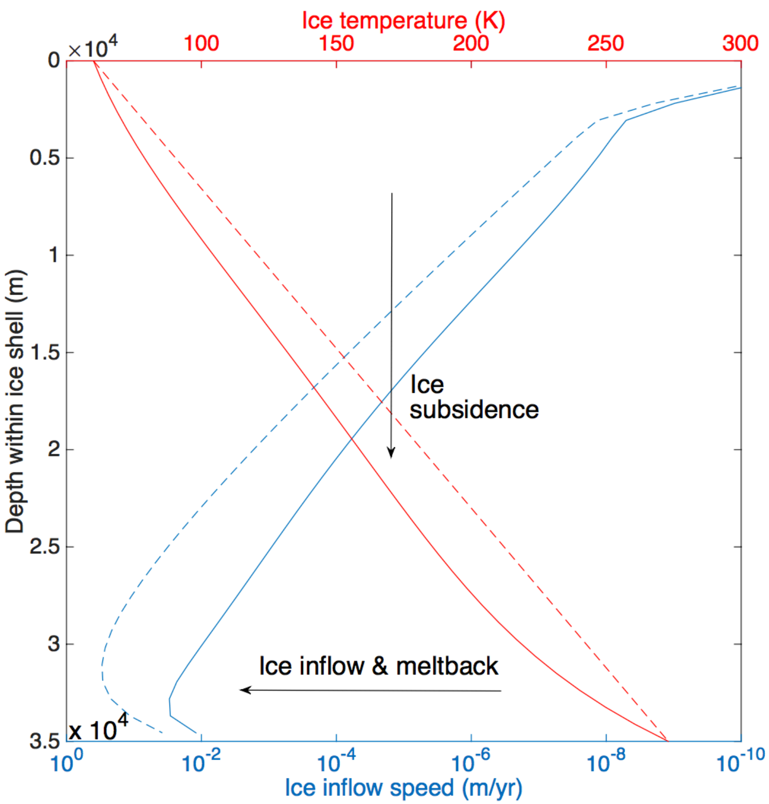

Kite & Rubin, Proc. Nat'l. Acad. Sci., 2016

Wet-based ice sheets

Basal melt

Applications: ice streams
will Greenland + Antarctic ice shelf collapse take a few millenia or a few centuries?

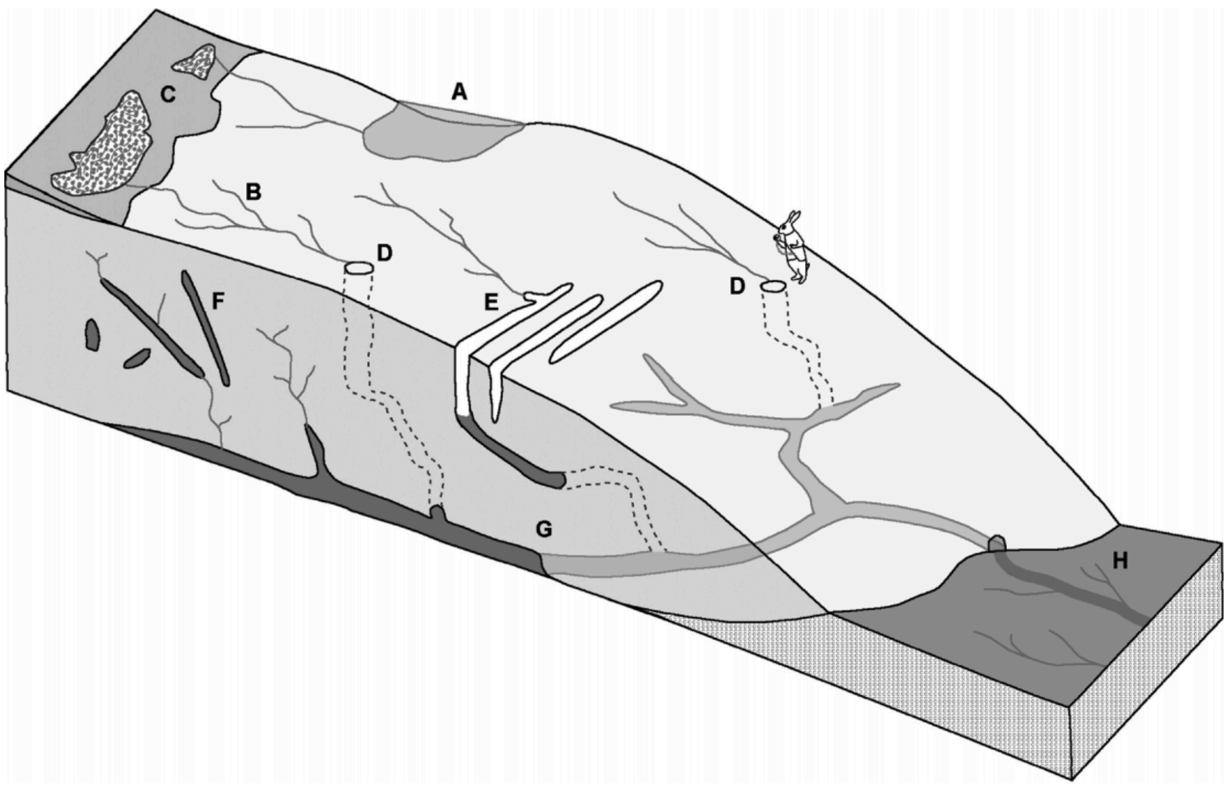

Figure 6.1: Some elements of the glacier water system: (A) Supraglacial lake. (B) Surface streams. (C) Swamp zones near the edge of the firn. (D) Moulins, draining into subglacial tunnels (for scale, white rabbit is about 10 m tall). (E) Crevasses receiving water. (F) Water-filled fractures. (G) Subglacial tunnels, which coalesce and emerge at the front. (H) Runoff in the glacier foreland, originating from tunnels and also from upwelling groundwater. Though not depicted here, water is also widely distributed on the bed in cavities, films, and sediment layers. Sediment and bedrock beneath the glacier contain groundwater. (Refer to the insert for a color version of this figure)

Eskers:

sand+gravel ridges deposited from subglacial water channels

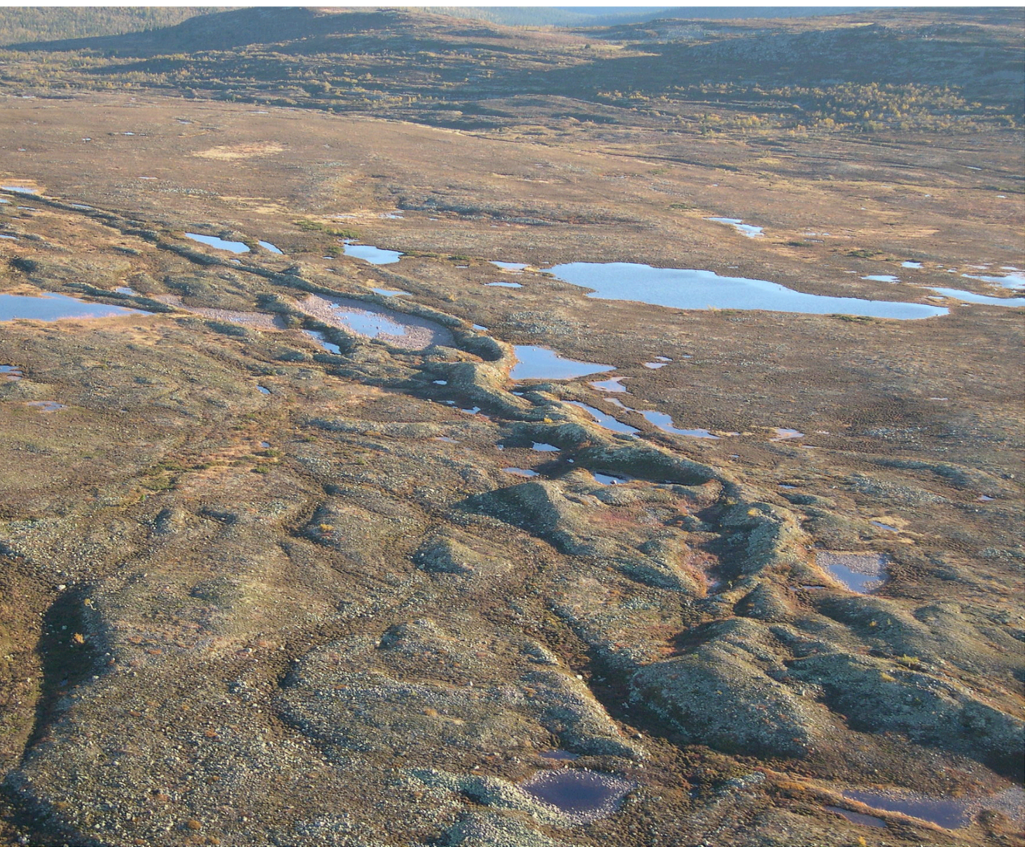

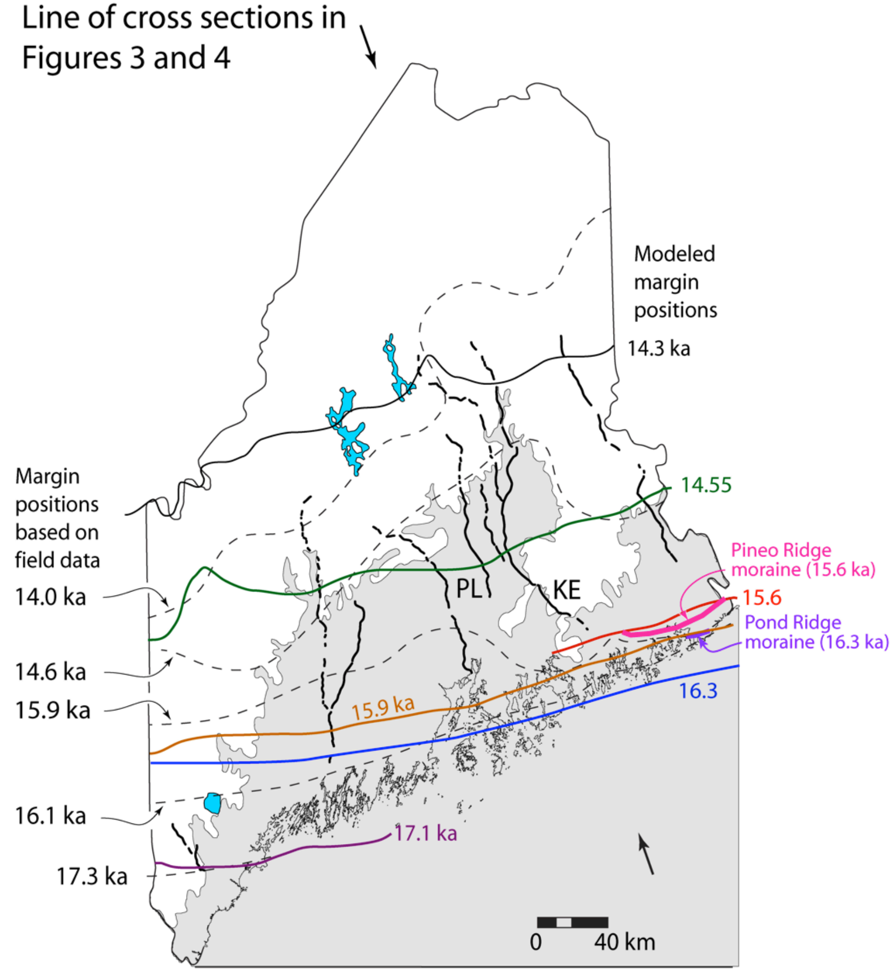

Katahdin esker system, Maine

Eskers can flow uphill: why?

How are subglacial conduits kept open?
Viscous inflow of warm ice will seal conduits near the ocean interface in decades, unless opposed e.g. Rothlisberger 1972

Nye (1953) / Rothlisberger (1972) theory for subglacial conduits

applications: plumbing system of cryovolcanoes on Enceladus and Ceres

Assume: water temperature = ice temperature

$$\frac{1}{R_c}\frac{\partial R_c}{\partial t} = A\left[\frac{N}{n}\right]^n \quad \text{with} \quad N = P_i - P_w$$

pressure driving closure

A,n: creep parameters for ice

$$\boxed{G = \frac{dP_w}{ds} + \rho_w\, g\, \sin\theta}$$

work done per unit volume of water per unit distance along flow

Energy required to raise water temperature (pressure dependence of the melting point of ice): $\rho_w c_w Q_w \mathcal{B}\, dP_i/ds$

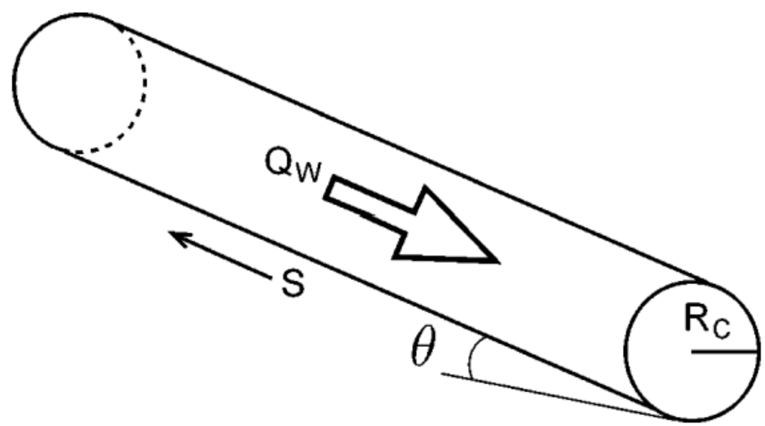

$$\dot{M}\,L_f = Q_w\,G - \rho_w\,c_w\,Q_w\,\mathcal{B}\,\frac{dP_i}{ds}$$

melt-back rate

heat generated by flow of water

warming of water

Following Cuffey, ch. 6., p.198-199 (suggested reading)

Pressure reduction in big Rothlisberger channels causes them to parasitize flow from smaller channels

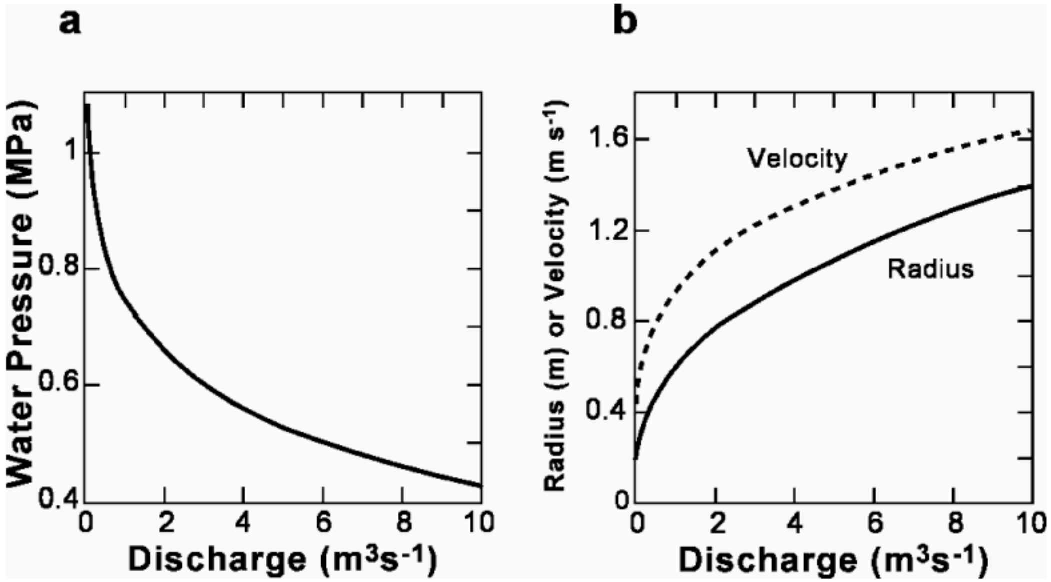

Figure 6.12: Predicted variation of water pressure, velocity, and radius for a tunnel in steady state, beneath 250 m of ice, with various discharges and one set of parameters ($\theta = 2.5°$, $A = 5 \times 10^{-24}$, $n_m = 0.1$).

Example: Mars, Dorsa Argentea Formation eskers (~3.5 Ga)

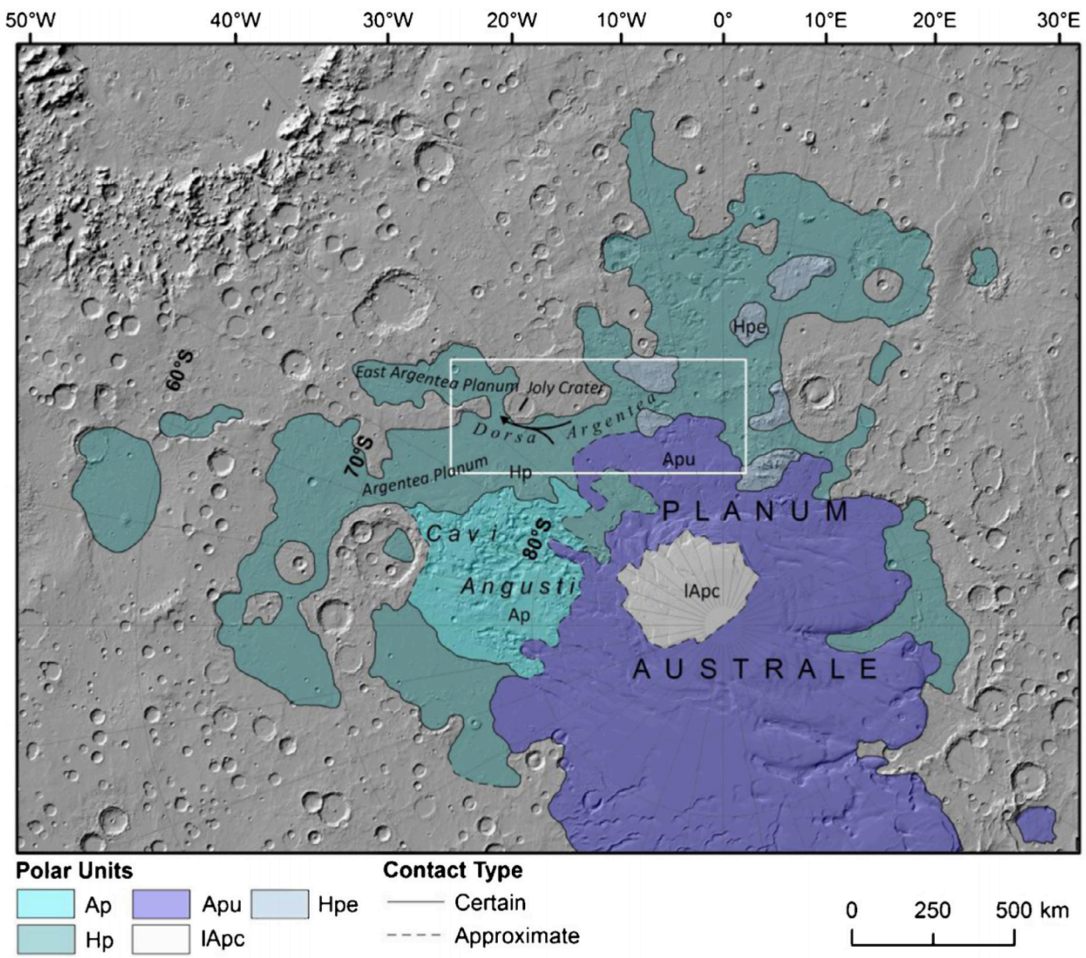

Butcher et al. Icarus 2016 – South Pole of Mars

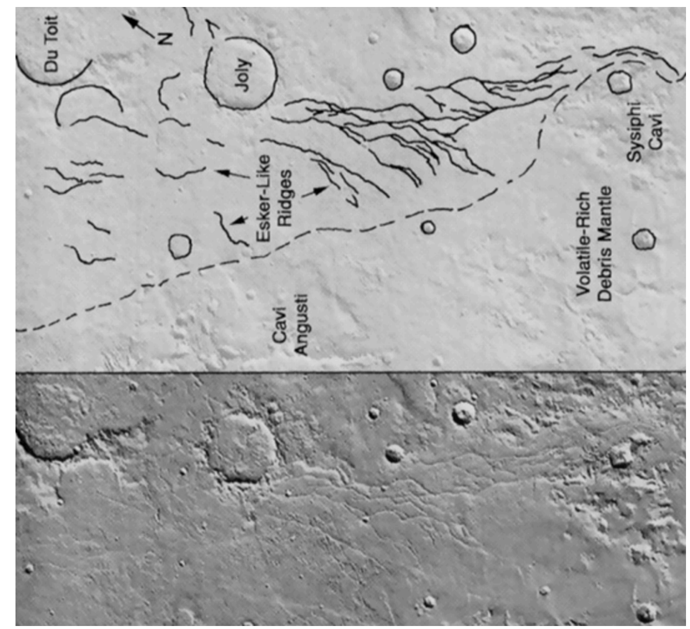

Fastook et al. Icarus 2012

The flow of ice

ICE MOVEMENT – GLEN'S LAW

TEMPERATURE STRUCTURE WITHIN ICE SHEETS – ESKERS (Mars examples)

EFFECT OF GLACIAL EROSION ON TOPOGRAPHY

(Earth examples)

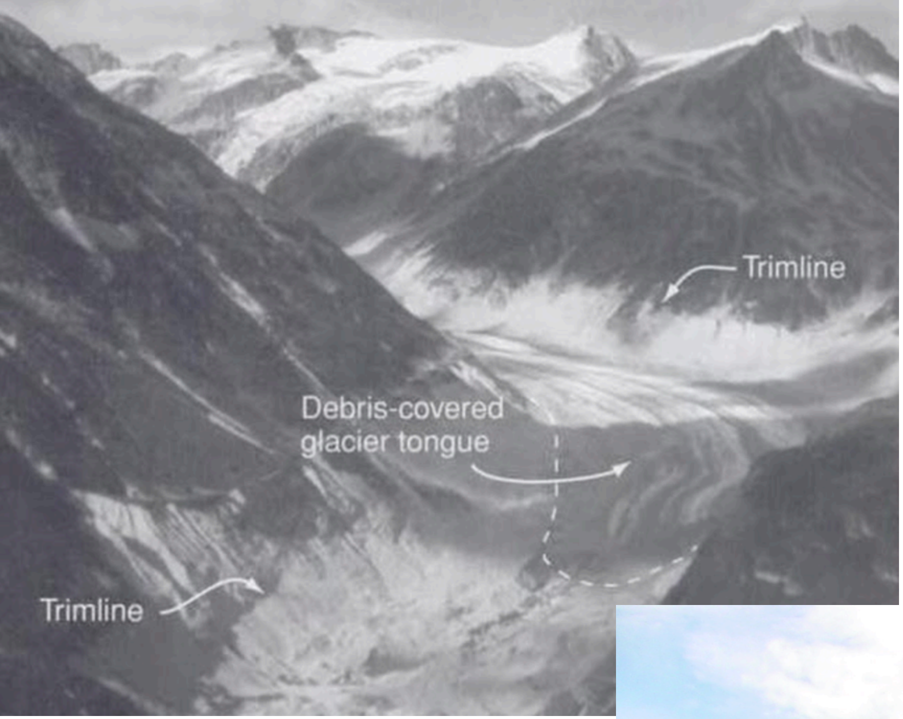

Trimline
Debris-covered
glacier tongue
Trimline

Origin of U-shaped glacial valleys: role of water table

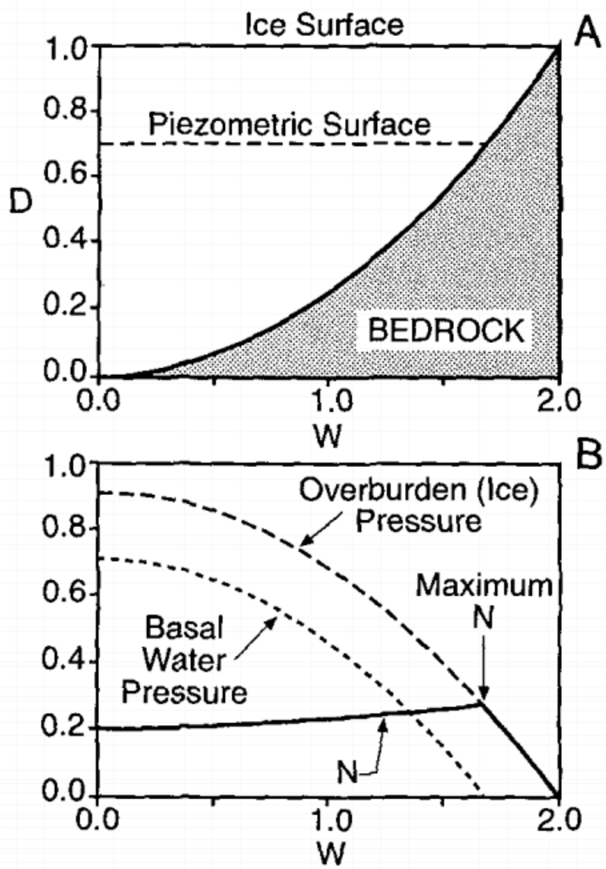

Figure 3. Effective normal stress distribution for a glacier with a parabolic cross section. Part A is a section through one-half of a glacier with a parabolic bed profile and a horizontal piezometric surface. D and W are dimensionless vertical and horizontal distances, respectively, from the low point of the section. Part B shows the distribution of the effective normal stress (N) for this section, where N is simply the overburden pressure minus the basal water pressure. Note that N increases rapidly away from the glacier margin to a maximum value, and then decreases progressively toward the center of the section.

Harbor, 1992, GSA Bulletin

Glacial abrasion and plucking scales as (sliding velocity)^2

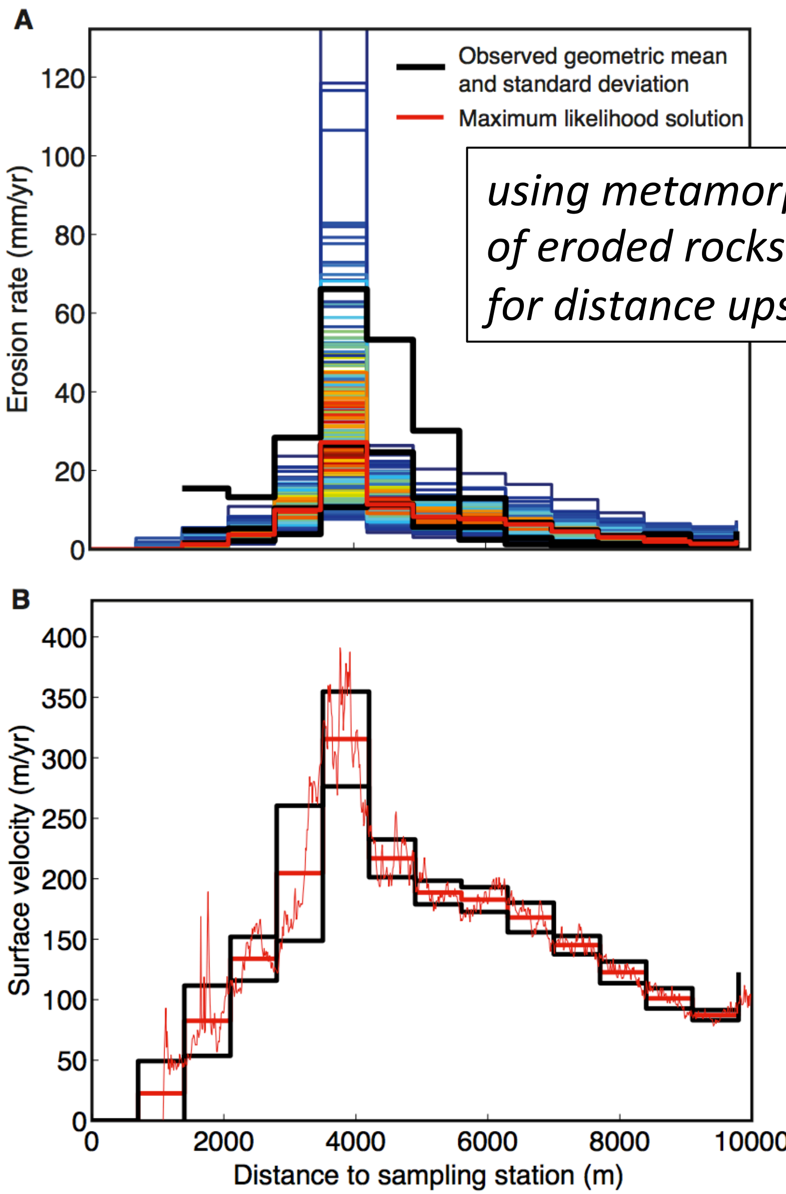

using metamorphic grade of eroded rocks as a proxy for distance upstream

Herman et al. Science 2015

Abrasion, quarrying

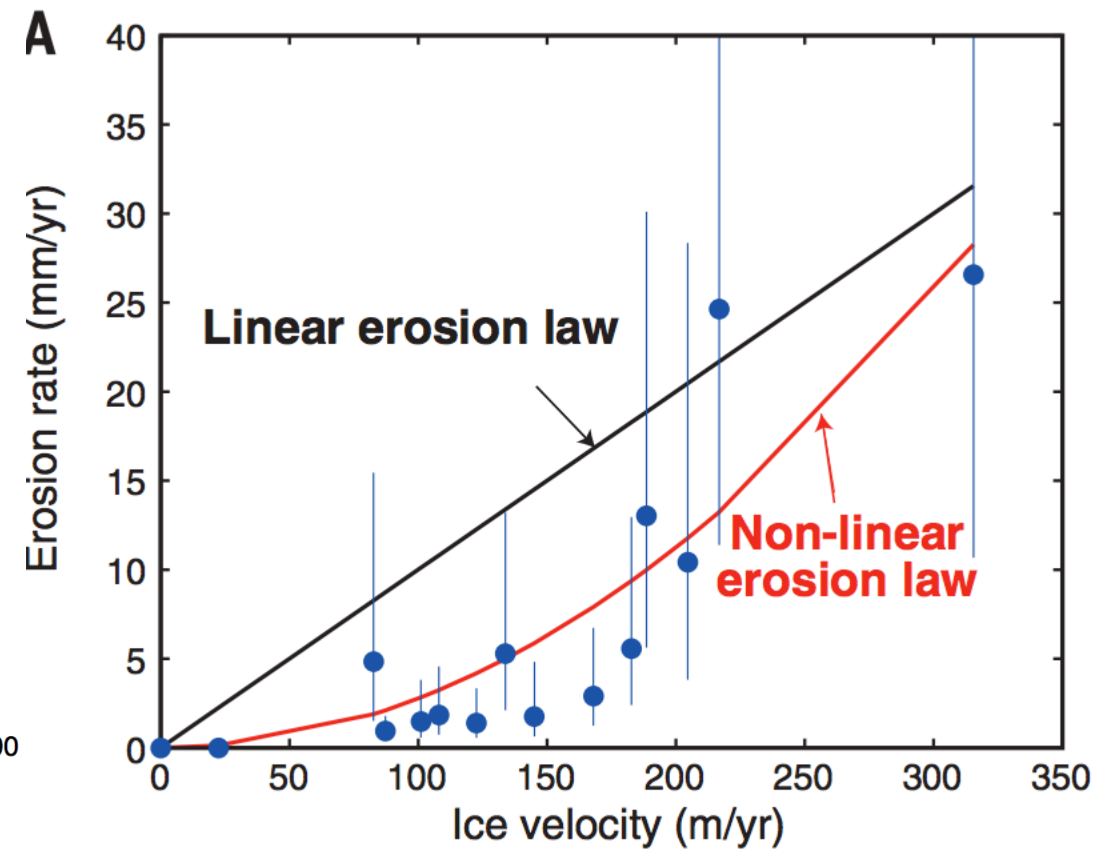

Global increase in erosion rate in the last 2 Myr – possibly due to increase in glaciation

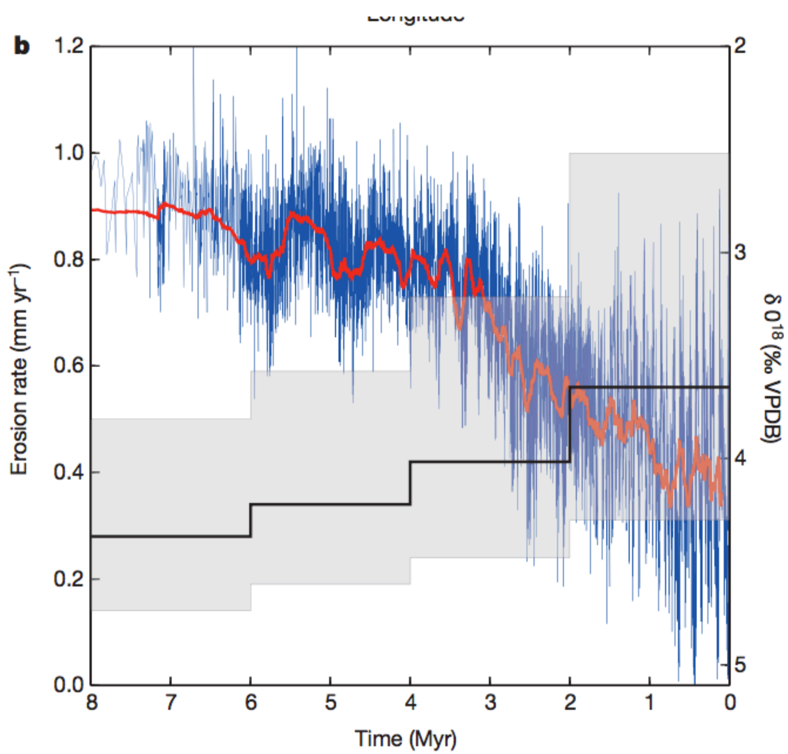

Figure 3 | Mountain erosion rates and δ^{18}O measurements during the Late Cenozoic era. **a**, Resolution is higher than 0.25 for the past 2 Myr. **b**, Erosion rate is computed at locations shown in **a**. The median (black line) and standard deviation (grey area) are estimated from the distributions of erosion rates over each 2-Myr time interval. (There is no weighting correction for areal coverage, except from using the solution at the grid points; see Methods.) The blue line depicts the raw δ^{18}O data compilation[11], whereas the red line corresponds to the moving average. VPDB, the Vienna Pee-Dee belemnite standard.

Herman et al. Science 2013
(thermochronology compilation)

Key points from today's lecture

- Glen's Law
- Approximations to the full Stokes equation: locations where they are and are not acceptable
- Nondimensional T-vs-depth as a function of accumulation rate for fixed basal heat flow
- Glacial erosion parameterization